

Femtosecond laser processing of evanescence field coupled waveguides in single mode glass fibers for optical 3D shape sensing and navigation

Christian Waltermann^{a,b}, Anna Lena Baumann^{a,b}, Konrad Bethmann^c, Alexander Doering^{a,b},
Jan Koch^a, Martin Angelmahr^a, and Wolfgang Schade*^{a,c}

^aFraunhofer Heinrich Hertz Institute, Am Stollen 19B, 38640 Goslar, Germany;

^bPhotonik Inkubator GmbH, Hans-Adolf-Krebs-Weg 1, 37077 Göttingen, Germany;

^cClausthal University of Technology, IEPT, Am Stollen 19B, 38640 Goslar, Germany

ABSTRACT

Fiber Bragg grating based optical shape sensing is a new and promising approach to gather position and path information in environments where classical imaging systems fail. Especially a real-time in-vivo navigation of medical catheter or endoscope without any further requirements (such as the continuous exposure to x-rays) could provide a huge advantage in countless areas in medicine.

Multicore fibers or bundles of glass fibers have been suggested for realizing such shape sensors, but to date all suffer from severe disadvantages.

We present the realization of a third approach. With femtosecond laser pulses local waveguides are inscribed into the cladding of a standard single mode glass fiber.

The evanescence field of the main fiber core couples to two S-shaped waveguides, which carry the light to high reflective fiber Bragg gratings located approx. 30 μm away from the centered fiber core in an orthogonal configuration. Part of the reflected light is coupled back to the fiber core and can be read out by a fiber Bragg grating interrogator. A typical spectrum is presented as well as the sensor signal for bending in all directions and with different radii. The entire sensor plane has an elongation of less than 4 mm and therefore enables even complicated and localized navigation applications such as medical catheters. Finally a complete 3D shape sensor in a single mode fiber is presented together with an exemplary application for motion capturing.

Keywords: Femtosecond Laser Processing, Fiber Bragg Grating, Cladding Waveguide, Fiber Optical Shape Sensor

1. INTRODUCTION

In 2003 Mazur et. al. [1] recognized a refractive index change of transparent glass substrates due to irradiation with focused ultra-short laser pulses for the first time. Since then, this effect has been successfully utilized for the direct processing of waveguides [2] and the creation of fiber Bragg gratings (FBGs) [3]. Today this so called point-by-point (PBP) inscription has evolved to a well-known and flexible tool for optical sensor systems.

Especially for FBGs femtosecond laser pulses offer various advantages compared to other FBG processing techniques. PBP inscribed Bragg gratings need no pre- or postprocessing which makes the resulting strain or temperature sensor extremely easy to handle and durable against mechanical stress. Other FBG production processes, such as the usage of a phase mask and an ultra violet laser [4], typically require the removal of the fiber coating and the application of a new protective layer afterwards. Furthermore by PBP technology, every point of a grating is created by a separate laser pulse or pulse train. This allows the creation of even complex grating geometries. Practically all known FBG types, like apodised, chirped, superimposed [5] or phase shifted gratings [6] have been realized with PBP writing.

Typical standard single mode fibers have a germanium doped core and a pure silica cladding. As the refractive index modification occurs in both materials, the cladding of a standard glass fiber can be manipulated with femtosecond laser pulses as well as its fiber core. We present, that with the PBP technique, actual cladding waveguides (CWG) with integrated FBGs can be inscribed anywhere in the cladding and evanescently couple to the fiber core. Several unique new sensor concepts can be implemented with such FBGs and a tremendous new potential for miniature optical devices and sensor systems, a complete "Lab in a Fiber", unfolds.

In the first part of this paper a flexible and reproducible way to inscribe waveguides and FBGs into the cladding of standard single mode glass fibers is presented. A basic characterization of these waveguide structures and FBGs within

the cladding follows. The reflectivity and the polarization dependency of CWG-FBGs have been measured and numerical simulations allow an approximation of the coupling efficiency between fiber core and waveguide. At the end of this part the accuracy of detecting a curvature with a CWG-based sensor will be estimated. In the last section, two applications of this new sensor concept will be presented: a complete 3D shape sensor integrated in one standard single mode fiber and a CWG-FBG fiber used to monitor human motion.

2. PROCESSING CLADDING WAVEGUIDES WITH FBG

A commercial Titanium:Sapphire regenerative amplifier system (seed laser Tsunami, amplifier Spitfire Pro F-XP, both from SpectraPhysics) is used to inscribe the waveguides as well as the FBGs into the fibers. The CWGs are processed with approx. 140 nJ pulse energy and the FBG with approx. 300 nJ. For both processing steps femtosecond laser pulses are focused into the fiber cladding with a high NA microscopic objective. An external Pockels cell is applied to attenuate the pulses and to reduce the repetition rate of the amplifier for the FBG inscription. To compensate the curved surface of the coating, the fiber is covered in an immersion fluid. XYZ nano positioners are used to move the fiber on predefined S-shaped trajectories in relation to the focal spot of the laser to create the waveguide and afterwards the FBG. A single line of femtosecond laser modifications resembles a gaussian refractive index profile. In order to minimize the bending losses (a later 3D shape sensor for medical applications has to be capable of detecting curvatures with radii below 1 cm) of the CWG an index step profile is best suited [8]. Therefore, a bundle of 20 overlapping lines is inscribed to create a waveguide with a circular index step profile and a diameter of approx. 5.7 μm . The resulting structure, as shown in Fig. 1, is very homogeneous and the surrounding cladding material suffers no visible damage due to the process. The almost identical contrast of fiber core and the waveguide bundle indicates an effective refractive index modification of the CWG in the same order of magnitude as the fiber core (in this case 0.0013). The chosen multi line approach of processing waveguides allows a very narrow gap between waveguide and fiber core, which is necessary for strong evanescent coupling.

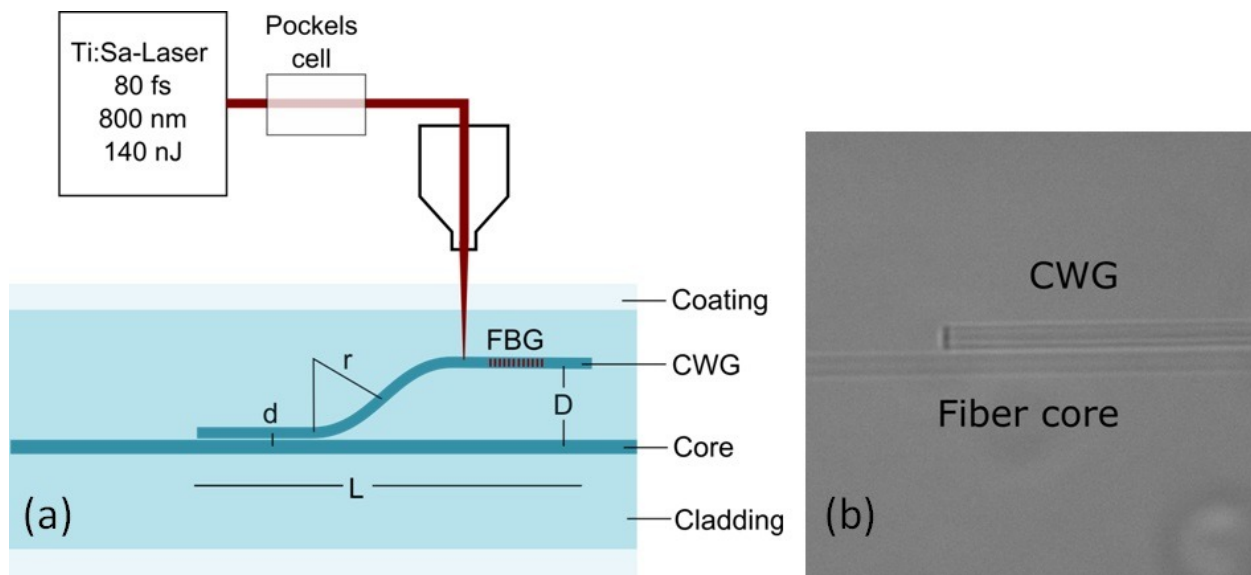


Figure 1. (a) Experimental setup for the inscription of cladding waveguides (CWG), (b) microscopic image of the beginning of a CWG next to the fiber core.

Fig. 2 shows a typical reflection and transmission spectrum of a CWG-FBG located 30 μm away from the fiber core in the cladding. The inscribed FBG has a length of 1 mm and a reflectivity of 20%. To obtain the transmission spectrum the fiber has been cut off and polished at the end of the CWG which was then connected to the fiber core of another single mode fiber. The significant losses for smaller wavelengths are typical for high reflective PBP created FBG. Additionally, laser inscribed gratings show a birefringence and therefore a small polarization dependant wavelength shift due to the elliptical shape of the laser focus. Identical to typical PBP processed FBG in a fiber core [9] the birefringence of a CWG-FBG has been determined to 3.0×10^{-5} . No further polarization dependant effects occur in the FBG signal.

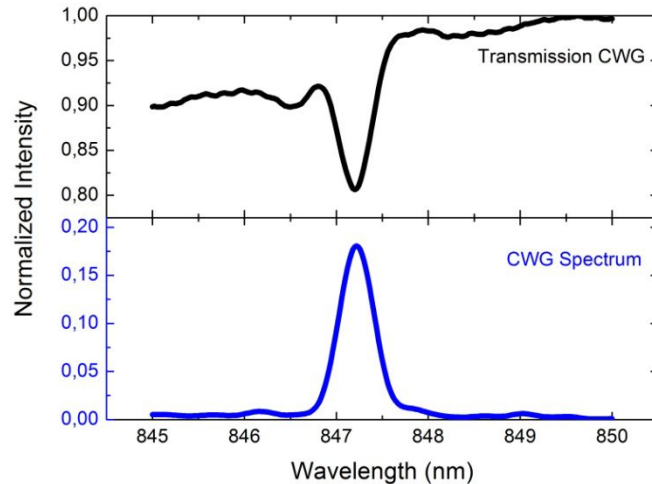


Figure 2. Typical spectrum of a FBG in the cladding of a standard single mode fiber.

3. SIMULATION OF INTENSITY IN CLADDING WAVEGUIDES

The evanescence coupling between fiber core and CWG is one of the most important factors for the successful implementation of a single fiber 3D shape sensor. To estimate the coupling strength intensity profiles for a set of geometrical parameters are presented. The simulation tool BeamPROP from SYNOPSIS Optical Solutions was used for the simulations. There are three different scenarios where coupling from or to the CWG can occur: the first is when light originating directly from the light source at the end of the fiber reaches the coupling region (Fig. 3(a)), the second when light reflected from the FBG in the CWG couples back into the fiber core (Fig. 3(b)) and the third when light reflected by other FBGs further down the fiber travels back and again passes the coupling region (Fig. 3(c)).

For the simulations a model of the system, consisting of fiber core, CWG, and surrounding cladding is created. The gap between the fiber core and the CWG is set to $d = 1 \mu\text{m}$, the wavelength of the guided light to 850 nm, the fiber core diameter to $5.7 \mu\text{m}$ and the CWG diameter to $6 \mu\text{m}$.

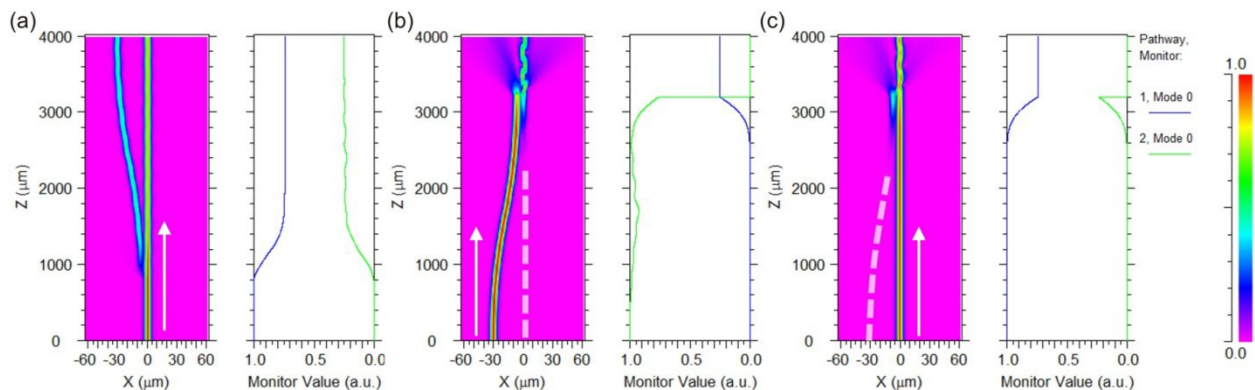


Figure 3. Intensity distribution and profiles of three different coupling scenarios with (a) the light coming from the light source, (b) light coming back from the FBG in the CWG and (c) light coming back from further towards the fiber end; white arrows indicate the light propagation and the white dashed lines the fiber core or CWG where not visible due to low intensity (color online).

The intensity distribution and profiles are shown in Fig. 3. In Fig. 3(a) part of the light from the light source couples into the waveguide going off to the left side. The slight meandering that can be observed is due to the fact that the CWG diameter is slightly different from the fiber core diameter, leaving the mode to adjust over some distance. While here the intensity profile of the CWG (right green line in the graph of Fig. 3(a)) follows the fluctuation, 25% of the input power are successfully coupled into the CWG and guided to the CWG-FBG.

In Fig. 3(b) the whole configuration is rotated by 180 degrees. It shows the light returning from the CWG-FBG coupling back into the fiber core with a much stronger meandering effect. This time however the fiber core intensity profile is unaffected and again approximately 25% of the power in the CWG is transferred back to the fiber core. Also, the graph displays nicely how the rest of the light is distributed into the cladding at the end of the CWG. Some slight intensity fluctuations can be seen during the curved part of the CWG but the power is recovered further towards the end of the CWG. Fig. 3(c) depicts how part of the light coming from FBGs situated further down at the end of the fiber is lost due to coupling into the end of the CWG close to the fiber core. As before 25% of the light is transferred to the CWG, then dumped in the cladding and slight meandering of the intensity distribution but not the intensity profile can be seen when the CWG mode interacts with the fiber core mode.

These simulations allow for a tentative evaluation of possible power losses of a shape sensor with two or more sensor levels. With 25% of the power coupling into the first CWG, 20% reflected by the CWG-FBG and 25% coupling back into the fiber core, we have only 1.25% coming back from the CWG-FBG to the interrogator. Considering that this value drops even lower the higher the number of sensor planes located between a CWG-FBG and the original light source, our experimental results with several successive sensor planes are remarkable. However, differences between our actual real life sensor and these simulations have to be considered: the refractive indices of CWG and fiber core may actually differ but are assumed the same in the simulations, distances may vary slightly due to optical distortion and other parameters may be influenced by process variables such as laser power fluctuations or contaminations in the immersion fluid surrounding the fiber.

4. CHARACTERISATION OF A CURVATURE SENSOR

The three-dimensional accuracy of a CWG-FBG-based shape sensor depends primarily on the wavelength accuracy of the applied FBG readout unit and the continuity of the sensor itself which means the accuracy of the three-dimensional detection principle. The quality of the 3D shape interpolation finally depends on the mechanical properties of the object intended to be measured.

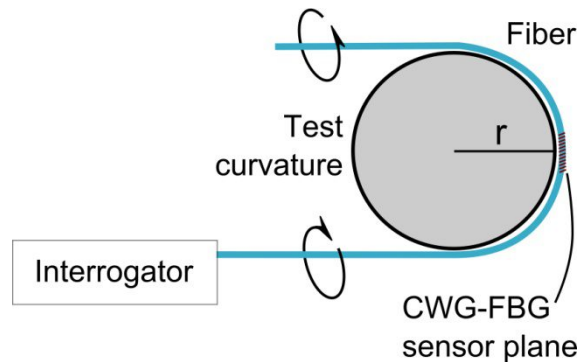


Figure 4. Setup for the characterization of a curvature sensor.

For a given system the accuracy of CWG-FBG-based shape sensors can be determined with the measurement setup pictured in Fig. 4. By rotating the three-dimensional shape sensor around a given constant curvature radius, an exact bend of the sensor plane in all directions can be implemented and the responding FBG data be acquired. This was done for three different radii, namely 6 cm, 7.7 cm, and 10 cm. To minimize torsion or other asymmetric effects during the rotation, the shape sensor was guided within a small tube filled with viscose oil and twisted symmetrically on both sides. The spectral signals of the CWG-FBG-based shape sensor have been analyzed during rotation by applying a FBG readout unit based on a spectrometer (Ocean Optics STS) and a broadband light source.

For the three different curvature radii, the recorded signals are depicted in Fig. 5(a) through (c). Two perpendicularly processed CWG-FBGs show an almost exact sinusoidal dependency between strain and bending direction. As shown in Fig. 5(d) the amplitude of the signals can be described with a $1/r$ characteristic which indicates that a CWG-FBG sensor responds to the stress induced by the applied curvature only. The relative wavelength shifts can be interpreted as the distance between fiber core and corresponding CWG in dependence of the applied bending radius. Therefore, the second CWG appears to be located in a slightly greater distance to the neutral axis of the fiber. Further, the phase shift between both CWG signals equals the geometric angle between the processed waveguides and can be fitted to 101 degrees for all three radii. This implies a CWG-FBG opening angle of 101 degrees, which was confirmed by a visual inspection of the

waveguide position with respect to the fiber core together with the slightly different distance to the fiber core of the end of the CWGs. A third FBG within the fiber core on the neutral axis stays virtually unchanged when the fiber is bend and is used to compensate external stress or temperature drifts of the sensor plane.

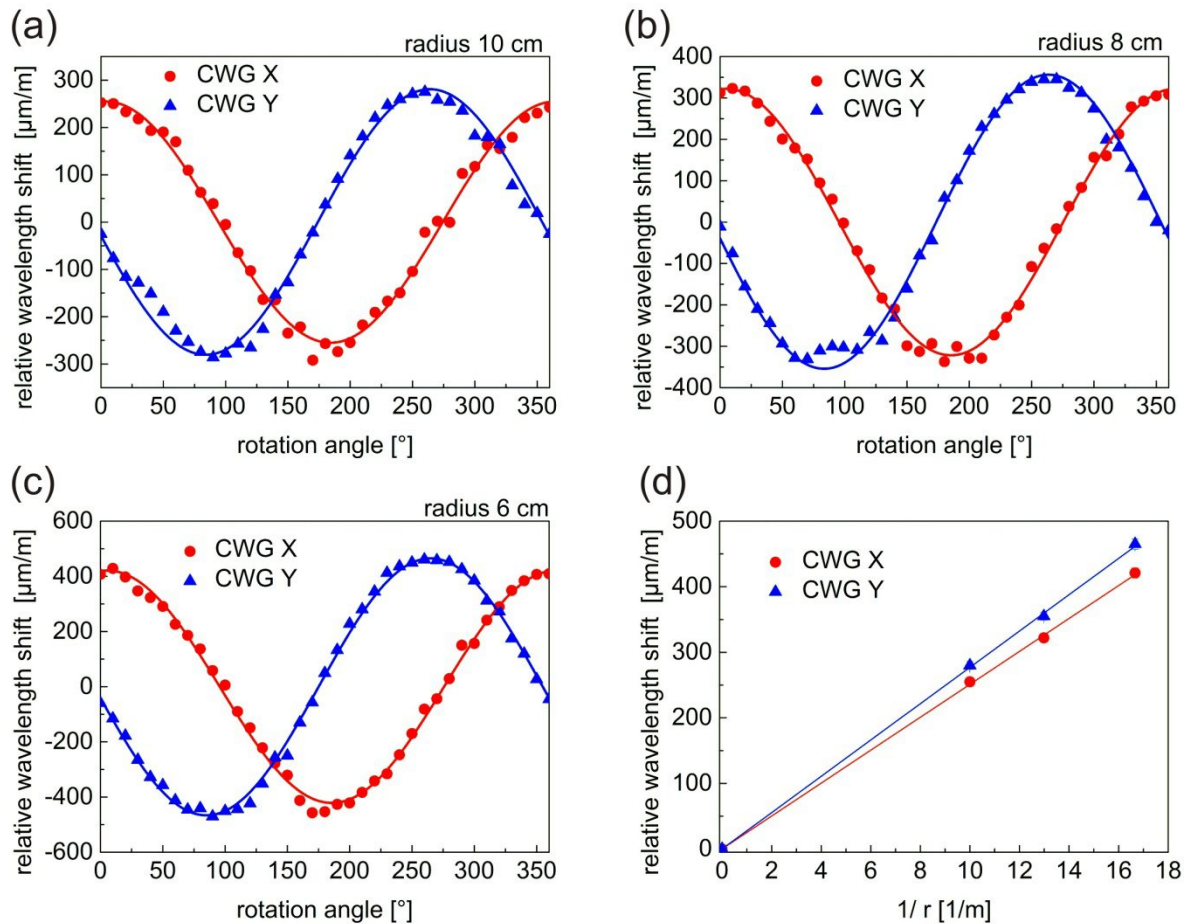


Figure 5. (a-c) Strain signals of CWG-FBG in dependency of the bending direction for three different radii, (d) maximum wavelength shift over reciprocal bending radius.

5. APPLICATIONS: 3D SHAPE SENSING AND MOTION CAPTURING

The results presented in the previous parts of this paper offer a wide range of possible applications. In this section exemplary applications in the two highly interesting fields of medical science and motion sensing are presented.

Using one single standard single mode fiber for 3D shape sensing overcomes the disadvantages of other previously proposed solutions. No custom made, complicated, and therefore expensive fan out device, which has to be used with multicore fibers [10], has to be integrated with each sensor and the fiber maintains its small diameter and flexibility compared to a fiber bundle [11].

For an actual 3D shape sensor that allows integration in a medical device like a catheter or endoscope [12], a number of CWG-FBG planes are necessary. The femtosecond laser process can create CWGs with arbitrary and extremely small coupling efficiencies. The spectrum of a complete 3D shape sensor consisting of 10 CWG-FBGs and therefore 5 curvature sensor planes is shown in Fig. 8. One additional core FBG (at a wavelength of 807 nm) is used to compensate global influences on the fiber. A distance of 2 cm lies between each curvature sensor plane and the fiber used is polyimide coated with a diameter of less than 150 μm . With such a small diameter, the sensor enables integration in even extremely small guide wires like the ones used for cardiac or brain catheters. A simple linear interpolation algorithm between the measured curvatures is employed to recalculate the 3D shape of the fiber. The fiber allows the

detection of radii well below 2.5 cm. In the top right corner of Fig. 6 a real-time image of a 3D recalculation of the fiber is shown.

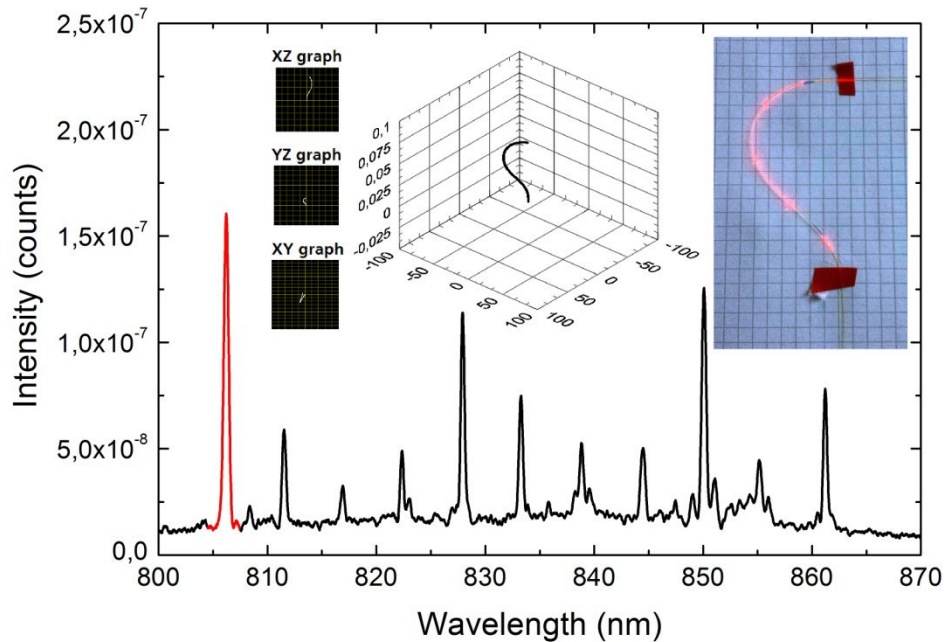


Figure 6. Spectrum of a 3D shape sensor with 5 curvature sensor planes and one FBG in the fiber core for temperature and stress compensation; inlays are in the top right corner a photograph of the fiber at a bending radius of approx. 2.5 cm (squares measure $5 \times 5 \text{ mm}^2$) and in the middle the corresponding 3D reconstruction.

A shape sensing demonstrator for real-time motion capturing was conceived to demonstrate another one of the endless application possibilities of this technology: the steering of a robot by using a 3D shape sensing fiber. Pictures of the robot and a fiber optically equipped test person can be seen in Fig. 7.



Figure 7. Fiber optically controlled robot with the robot's right arm being steered by a test person's left arm

The robot's right arm is controlled by the left arm of the test person. The two pictures in Fig. 7 show the closing and opening of the robot's hand. In the left picture the robot is holding a small ball, notice the test person's hand in the exact same position. In the right picture the test person's hand has been released causing the robot to drop the ball. For this application the test person's arm is equipped with four sensors, one for each joint of the arm. The first one is situated at the finger, the following on a spiral around the forearm, the next at the elbow, and the last is located near the shoulder. With these sensors all arm movements are evaluated by adapted software. There is no need for interpolation in between the different sensor planes as due to the stiffness of the human bones there is only minimal movement in between the joints. Therefore each sensor plane's curvature is the value that is used for further analysis. To obtain the corresponding arm positions the evaluation software needs to be calibrated. This is done by having the test person move his or her arm

to the extremal positions. In the case of the sensor for the elbow this would be the positions shown in Fig. 8(a) and 8(b), with the second being the minimal angle that the robot is able to bend its arm. For both positions the signals of the corresponding sensor plane are saved, enabling the software to recognize them and all intermediate positions like the one in Fig. 8(c). According to the current position of the human arm the software calculates the corresponding angle required for the robot's movements and sends it to the robot via a network interface. The process is the same for all four sensor planes, though the forearm sensor does not monitor the direct shape. As it is situated on a spiral it is used to keep track of the hand rotation against the elbow. The spiral opens and closes when the hand is rotated outward and inward respectively. The resulting change in the shape of the fiber is quite small, but the fidelity of the sensor is high enough to evaluate different hand rotations, and it can thus be used as a basic torsion sensor.

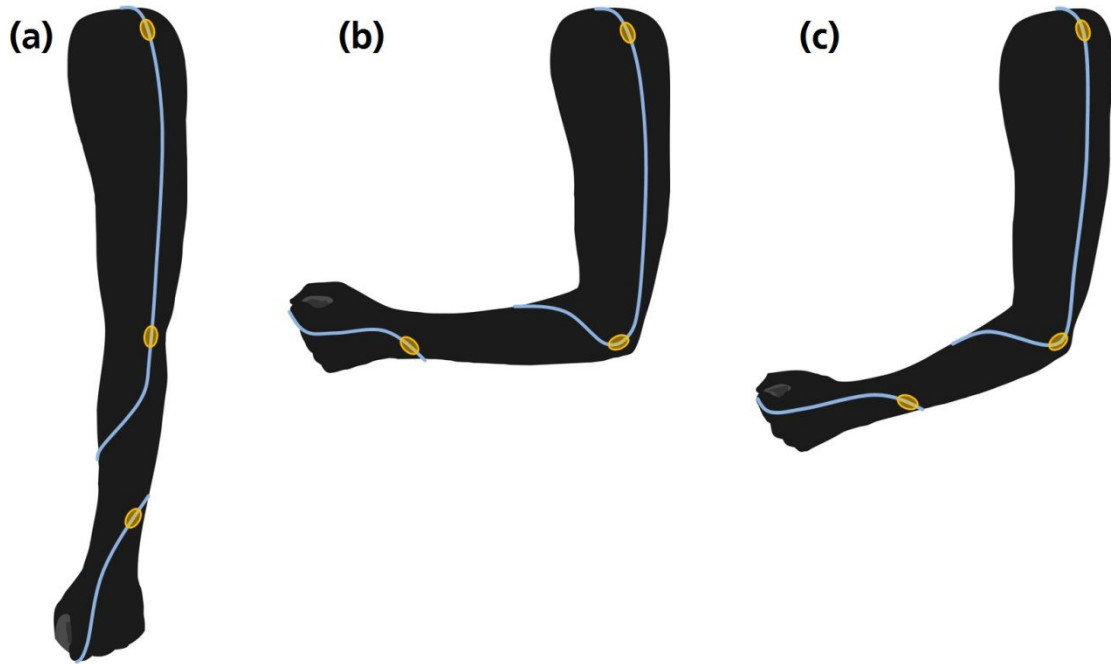


Figure 8. Schematic of a fiber optically equipped human arm, sensor positions on the fiber trail in light blue are marked in yellow (color online): (a) and (b) calibration positions for the elbow, (c) intermediate position.

6. CONCLUSION AND OUTLOOK

A novel approach to realize a purely fiber optical 3D shape sensor based upon cladding waveguides (CWG) and fiber Bragg gratings (FBGs) has been presented. Focused femtosecond laser pulses can be utilized to inscribe homogeneous waveguide structures into the cladding of a standard single mode fiber without removal of its protective coating. These CWG can couple to the evanescent field of the light propagating in the fiber core and the desired coupling efficiency can easily be achieved by optimizing geometric parameters found with numerical simulations. FBGs written into CWG structures behave identical to “classical” FBGs inscribed into a fiber core and therefore react to stress induced to the cladding by bending the fiber. Two perpendicular CWG structures are used to determinate the bending direction and radius of the fiber. Applying several sensor planes a three-dimensional recalculation of the fiber shape can be achieved.

This simple single mode glass fiber that is capable of detecting its own form can be integrated in nearly every possible environment and could therefore become a key element for countless applications in medicine, robotics or real time structural health and condition monitoring. On the way to a “Lab in a Fiber”, the possibility of using the entire cladding for sensory tasks offers an additional new and vast potential.

REFERENCES

- [1] Schaffer, C. B., Garcia, J. F., and Mazur, E., "Bulk heating of transparent materials using a high repetition-rate femtosecond laser," *Appl. Phys. A* 76, 351–354 (2003).
- [2] Hirao, K., and Miura, K., "Writing waveguides and gratings in silica and related materials by a femtosecond laser," *J. Non-Cryst. Solids* 239, 91 (1998).
- [3] Hill, K. O., Malo, B., Bilodeau, F., Johnson, D. C., and Albert, J., "Bragg gratings fabricated in monomode photosensitive optical fiber by UV exposure through a phase mask," *Appl. Phys. Lett.* 62(10), 1035 (1993).
- [4] Mihailov, S., and Gower, M., "Recording of efficient high-order Bragg reflectors in optical fibers by mask image projection and single pulse exposure with excimer laser," *Electronics Letters* 30, 707-708 (1994).
- [5] Williams, R. J., Voigtländer, C., Marshall, G. D., Tünnermann, A., Nolte, S., Steel, M. J., and Withford, M. J., "Point-by-point inscription of apodized fiber Bragg gratings," *Opt. Lett.* 36, 2988 (2011).
- [6] Burgmeier, J., Waltermann, C., Flachenecker, G., and Schade, W., "Point-by-point inscription of phase-shifted fiber Bragg gratings with electro-optic amplitude modulated femtosecond laser pulses," *Opt. Lett.* 39(3), 540-543 (2014).
- [7] Araújo, F. M., Ferreira, L. A., and Santos, J. L., "Simultaneous determination of curvature, plane of curvature, and temperature by use of a miniaturized sensing head based on fiber Bragg gratings," *Appl. Opt.*, 41(13), 2401-2407 (2002).
- [8] Sakai, J., and Kimura, T., "Bending loss of propagation modes in arbitrary index profile optical fibers," *Appl. Opt.* 17(10), 1499-1506 (1978).
- [9] Martinez, A., Dubov, M., Khrushchev, I., and Bennion, I., "Direct writing of fiber Bragg gratings by femtosecond laser," *Electron. Lett.* 40, 1170 (2004).
- [10] Thomson, R. R., Bookey, H. T., Psaila, N. D., Fender, A., Campbell, S., MacPherson, W. N., Barton, J. S., Reid, D. T., and Kar, A. K., "Ultrafast-laser inscription of a three dimensional fan-out device for multicore fiber coupling applications," *Optics Express* 15(18), 11691-11697 (2007).
- [11] Waltermann, C., Koch, J., Burgmeier, J., Thiel, M., Angelmahr, M., and Schade, W., "Fiber Optical 3D Shape Sensing", in Marowsky, G., [Planar Waveguides and other Confined Geometries], Springer Series in Optical Sciences, Vol. 189 (2014).
- [12] Waltermann, C., Koch, J., Angelmahr, M., Schade, W., Witte, M., Kohn, N., Wilhelm, D., Schneider, A., Reiser, S., Feussner, H., "Femtosecond Laser Aided Processing of Optical Sensor Fibers for 3D Medical Navigation and Tracking (FiberNavi)," *Proc. SPIE* 9157, 23rd International Conference on Optical Fibre Sensors, 91577G (June 2, 2014).